Camera Vision and Inertial Measurement Unit Sensor Fusion for Lane Detection and Tracking using Polynomial Bounding Curves

Christopher Rose, *Auburn University*
David M. Bevly, *Auburn University*

BIOGRAPHY

Christopher Rose was born in Huntsville, Alabama. He is a member of the GPS and Vehicle Dynamics Lab at Auburn University and is pursuing a Master's Degree in Electrical Engineering. His current activities focus on video processing applications and sensor fusion in ground vehicles. He received his B.S. in Electrical Engineering at Auburn University in 2007.

David M. Bevly received his B.S. from Texas A&M University in 1995, M.S. from Massachusetts Institute of Technology in 1997, and Ph.D. from Stanford University in 2001 in mechanical engineering. He joined the faculty of the Department of Mechanical Engineering at Auburn University in 2001 as an assistant professor. Dr. Bevly's research interests include control systems, sensor fusion, GPS, state estimation, and parameter identification. His research focuses on vehicle dynamics as well as modeling and control of vehicle systems. Additionally, Dr. Bevly has developed algorithms for navigation and control of off-road vehicles and methods for identifying critical vehicle parameters using GPS and inertial sensors.

ABSTRACT

This paper studies a technique for combining vision and inertial measurement unit (IMU) data to increase the reliability of lane departure warning systems. In this technique, 2nd order polynomials are used to model the likelihood area of the location of the lane marking position in the image as well as the lane itself. An IMU is used to predict the drift of these polynomials and the estimated lane marking when the lane markings can not be detected in the image. Subsequent frames where the lane marking is present results in faster convergence of the model on the lane marking due to a reduced number of detected erroneous lines.

A technique to reduce the affect of untracked lane markings has been employed which bounds the previously detected 2nd order polynomial with two other polynomials within which lies the likelihood region of the next frame's lane marking. These bounds employ similar characteristics as the original line; therefore, the lane marking should be detected within the bounded area given smooth transitions between each frame.

An inertial measurement unit can provide accelerations and rotation rates of a vehicle. Using an extended Kalman filter, information from the IMU can be blended with the last known coefficients of the estimated lane marking to approximate the lane marking coefficients until the lane is detected. A measurement of the position within the lane can be carried out by determining the number of pixels from the center of the image and the estimated lane marking. This measurement value can then be converted to its real world equivalent and used to estimate the position of the vehicle within the lane.

INTRODUCTION

Many navigation systems combine an IMU and GPS in order to determine the location of a vehicle. The IMU provides high data rates at the cost of integration drift while GPS provides more accurate measurements at slower rates. Similarly, cameras provide passive, accurate measurements at lower rates. At low velocities, cameras can track very accurately, but higher speeds create motion blur and limitations of camera sampling rates [8]. Inertial sensors, however, have large measurement uncertainty at slow motion and lower relative uncertainty at high velocities [8]. IMU's and cameras, then, are complementary, and each possesses their own respective strengths.

A common strategy for combining inertial and visual sensors is the structure from motion (SfM) problem, which estimates the 3-D position of points in the scene with respect to a fixed coordinate frame and the pose of the camera [8]. Features within the image are tracked from frame to frame, and the change in camera pose and

world coordinates for each feature is estimated. These features can be either points [28] or lines [24]. Ansar [2] presented a general framework for a linear solution to the pose estimation problem with points and lines. For 3-D reconstruction, the range to each point must be known, since slow moving objects nearby can appear to move at the same speed as far away fast moving objects. The most common approach to this problem is the use of stereo vision, where the differences in each image can be used to determine the distance to points in the image. For a single camera, 3D motion estimation can be determined over the course of multiple frames [6]. One limitation of an inertial/vision system using this technique is the need to track features across multiple frames. If a feature is not present within successive images, tracking fails and the system cannot estimate ego motion. As such, most inertial/vision systems have a limit with respect to motion at which they can operate. However, most applications involving inertial and vision systems, such as that of a mobile robot or robotic arm, do not approach this limit under normal conditions.

In this paper, a camera and IMU is integrated to more robustly determine location within a lane than vision alone. Many navigation systems desire lane level positioning in difficult environments. Without differential GPS, lane level accuracy is difficult to achieve, especially in areas where satellites are blocked. Also, lane departures account for nearly 50% of all fatalities on the road. The force of two cars colliding head on is much greater than that of a car hitting a stationary object. When two cars collide in this manner due to a lane departure, this additional force is catastrophic on the car and on the occupants within. Camera-based detection of road markings is already a proven method of lane localization and can be found in commercial vehicles today. However, environments with many objects, such as urban environments, or even certain lighting conditions can cause problems for camera systems when detecting road markings. An IMU can provide information on the movement of the vehicle when lane markings are not detected.

One common feature extraction technique in lane departure warning systems is the use of the Hough transform, which extracts lines from an image. The detected lane marking lines can be used to interpolate a 2nd order polynomial to estimate the shape of the lane marking curve in the image. However, vision-only lane departure warning systems are limited by the quality of the frame image and the information contained within each frame. Blurry frames, adverse weather conditions, and shadows can ruin detection of lines. Additional road markings on the ground, such as that of a crosswalk, turn arrow, or merged lane, can introduce rogue lines into the image and shift the estimated lines beyond that of the actual lane markings. Dashed lane markings of the center road can reduce its detection rate and lead to gaps in the lane marking model for that frame. Other vehicles on the road, such as those found in an urban environment, and faint road markings can interfere with tracked lane markings. A Kalman filter whose states are the coefficients of the polynomial for the estimated lane marking can reduce the impact of erroneous detected lane marking lines; however, lane tracking is lost if the lane itself is unseen in the image or if an erroneous object (such as the edge of a car) is tracked as a lane. Since the 2^{nd} order polynomial is tracked from frame to frame rather than points or lines, lower resolution images can be employed with this system. Thus, the constant presence of lane markings in road images can be exploited in order to alleviate the need for points or lines that exist across multiple frames. As such, the speed at which the car moves forward is not a limitation of the system. The lateral velocity, however, must not be large enough to cause the lane model to leave the bounded area. More information about the vision system can be found in [25].

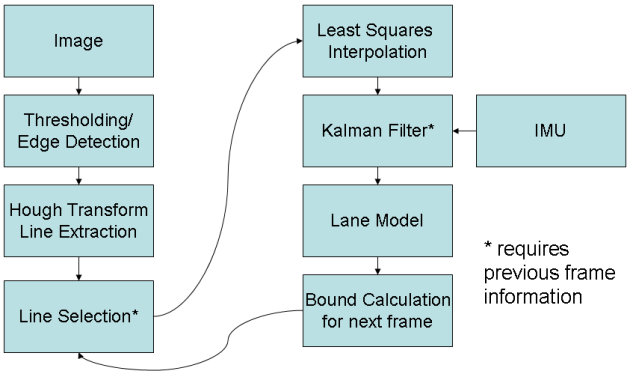

Figure 1: Overview of system

In this system shown in Fig. 1, the distance measured from the camera algorithm is used to update the lateral distance detected using the lateral accelerations from the IMU. The estimated distance the car has moved is then used to shift the lane model within the image to account for this change. Thus the lane model can be estimated even in situations where the lane is not detected or detected infrequently, such as that for dashed lane markings.

CAMERA LANE MEASUREMENT

The camera takes images of the road ahead and is currently mounted on the roof of the vehicle. The pinhole camera model is assumed; therefore, no skew or lens distortion is considered present in the images. Each lane marking is modeled using a 2^{nd} order polynomial – the coefficients of which are used for measurements of the extended Kalman filter.

To determine the coefficients for the left and right lane markings, each image is thresholded after having been

converted to a grayscale image and region of interest selected. This thresholding is used to eliminate the undesired features of the image. The "blobs" that remain within the image are indicative of the lighter pixels within the image, such as white or yellow lane markings. However, other, lighter objects within the image, such as road barriers, are present as blobs within the thresholded image as well. The objective is to find the blobs of the lane markings and ignore the blobs of the other features in the image. Edge detection converts these blobs into their defined edges.

Figure 2: Image on highway following edge detection

The Hough transform is a common technique for extracting lines within an image. Using the probabilistic Hough transform, the minimum line width and maximum gap between line segments can be set to further refine which lines are likely to be lane marking lines. Each of the detected lines is classified as left or right lane marking lines using their slope.

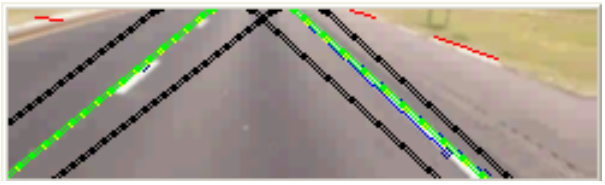

Figure 3: Road model and bounding curves on straight road (green – detected estimated road marking)

In typical road driving conditions, the location of the lane markings within the image will generally not change often. Due to this, the location of the lane marking in the last image should be relatively close to the location of the lane marking in the current image. Polynomial bounding curves are used to establish the region within the image where the lane marking lines are likely to be located. These curves are constructed from samples of points on the last lane model using the following equations:

$$x_{rightbound} = x_{est} + r\sin(\tan^{-1}(\frac{dy}{dx})_{est}) \quad (1)$$

$$y_{rightbound} = y_{est} - r\cos(\tan^{-1}(\frac{dy}{dx})_{est}) \quad (2)$$

$$x_{leftbound} = x_{est} - r\sin(\tan^{-1}(\frac{dy}{dx})_{est}) \quad (3)$$

$$y_{leftbound} = y_{est} + r\cos(\tan^{-1}(\frac{dy}{dx})_{est}) \quad (4)$$

where x_{est} and y_{est} are the x points and y points of the estimated lane model, r is the normal distance from the estimated lane model and the bounded line, and dy/dx is the slope at the (x_{est},y_{est}) point on the estimated lane model. These equations provide points on each boundary curve, which can then be used to approximate a 2nd order polynomial using least squares approximation. For each lane marking model, two of these boundary curves "bound" the last estimated lane marking and establish the region within the image that valid lane marking lines will be located. Lines which do not lie close to the last estimated lane marking are then ignored.

Similarly, the slope of the last estimated lane marking near the line in question should be similar to the current possible lane marking line. Each line that is detected within the boundary curves is compared in slope to the nearby slope of the last estimated lane marking, since a 2nd order polynomial has changing slope. This process eliminates erroneous lines that fully lay within the boundary curves.

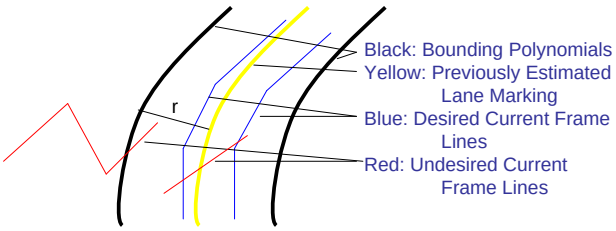

Figure 4: Line Selection – Slope and Bounds

Despite these two strategies for eliminating erroneous lines as candidates for the estimated lane line, very noisy images may still have erroneous lines and cause the estimate of the lane marking to drastically move away from the line. In addition, multiple, valid line candidates on the lane marking create a situation where all valid lines should be incorporated into the solution. A least squares polynomial approximation is conducted on the endpoints and midpoints of all candidate lines to reduce the effect of erroneous lines, incorporate multiple valid lines, and convert the model into coefficient form. For situations where each side of a lane marking is detected, the least squares solution of the estimated polynomial will result in an estimate that lies within the actual lane marking within the image, rather than its edges. The coefficients that arise from the least squares approximation are used in the measurement update of the coefficients.

$$\beta = (f'f)^{-1} f'y \quad (5)$$

where

$$f = \begin{bmatrix} 1 & x_1 & x_1^{\,2} \\ 1 & x_2 & x_2^{\,2} \\ \vdots & \vdots & \vdots \\ 1 & x_{n-1} & x_{n-1}^{\,2} \\ 1 & x_n & x_n^{\,2} \end{bmatrix} \quad (6)$$

$$y = \begin{bmatrix} y_1 \\ y_2 \\ \vdots \\ y_{n-1} \\ y_n \end{bmatrix} \quad (7)$$

$$\beta = \begin{bmatrix} c & b & a \end{bmatrix} \quad (8)$$

for

$$y_{est} = a x_{est}^{\,2} + b x_{est} + c \quad (9)$$

where $x_1, x_2, \ldots, x_n$ are x values and $y_1, y_2, \ldots, y_n$, are y values from each point.

Once the estimation for the lane marking model is found, an estimate for the distance of the vehicle to the right lane marking is calculated. The following equations use the general form of the quadratic equation to determine the point on the lane model polynomial with respect to any height within the image.

$$d_{right} = n\left(\frac{-b + \sqrt{4ay + b^2 - 4ac}}{2a} - x_{cam}\right) \quad (10)$$

$$d_{left} = n\left(x_{cam} - \frac{-b - \sqrt{4ay + b^2 - 4ac}}{2a}\right) \quad (11)$$

where a, b, and c are the coefficients of the estimated polynomial model, y is the row in the image at which the measurement should take place, n is the conversion factor, and x_{can} is the center of the image.

The bottom row of pixels is chosen as the row to measure the distance to either lane, since it has the most resolution with respect to the road. The converted distance is subtracted by the initial location of the vehicle (which is assumed to be known) in the lane and used in the measurement update to update the distance state.

More information on the lane estimation can be found in [25].

KALMAN FILTER STRUCTURE

The states of the filter are as follows:

$$\hat{x} = \begin{bmatrix} a_L \\ b_L \\ c_L \\ a_R \\ b_R \\ c_R \\ y \\ \dot{y} \\ b_y \\ \psi \\ \dot{x} \end{bmatrix} \quad (12) \qquad u = \begin{bmatrix} \ddot{x} + b_x \\ \ddot{y} + b_y \\ \dot{\psi} + b_\psi \end{bmatrix} \quad (13)$$

where $a_L, b_L, c_L, a_R, b_R, c_R$ are the coefficients of the measurement of the left and right lane models from the camera, y is the lateral position, $\dot{y}$ is the lateral velocity, $\dot{x}$ is the longitudinal velocity, ψ is the yaw, and b_y is the bias of the lateral acceleration. Two assumptions are made about the IMU states: the yaw rate, $\dot{\psi}$, has no or little bias, and the longitudinal acceleration, $\ddot{x}$, has a bias that is updated using another sensor other than the camera, such as a speedometer or wheel speed sensor. Since the method of extracting features within the image uses a model for the lane marking as the means of extracting the distance from the right lane with the camera, the camera cannot be used to update the state for longitudinal velocity with the current camera algorithm. The lane model has no means of tracking objects within the image that are parallel with the lane markings. Another sensor must be used, or the bias is assumed to be at a constant value. The IMU used in the experimental results, the XBOW 440, has little bias in its gyroscopes, which allows for the assumption of no bias for the yaw rate.

Measurements of the estimated lane model coefficients from the camera lane model determination are used to update the coefficient states. Bias of the lateral acceleration is updated using the lateral position estimate. An alternate structure to the above structure ignores the longitudinal acceleration and yaw rate from the IMU with the disadvantage of having no centripetal acceleration or lateral velocity component from forward acceleration due to zero yaw.

TIME UPDATE

The time update for the Kalman filter updates the lateral velocity, lateral position, yaw, longitudinal velocity, and coefficient states. The Runge-kutta method is used to update the lateral velocity, lateral position, yaw, and longitudinal velocity states. The following are the equations of motion:

$$\begin{aligned}
\dot{y} &= \dot{y}\cos(\psi) + \dot{x}\sin(\psi) \\
\ddot{y} &= u_0\cos(\psi) + u_2\sin(\psi) - b_y - \dot{y}u_1 \\
\dot{b}_y &= 0 \\
\dot{\psi} &= u_1 - 0 \\
\ddot{x} &= u_2\cos(\psi) + u_0\sin(\psi) - b_x
\end{aligned} \tag{14}$$

where u_0,u_1,u_2 are inputs as shown in Eq. (13), $\dot{\psi}$ is assumed to have no or very little bias, and b_x is assumed constant or updated with another sensor.

The coefficient update is updated in discrete time and is the change in each coefficient for a horizontal shift of a 2nd order polynomial.

$$\begin{aligned}
a_L &= 0 \\
b_L &= -2a_L m \\
c_L &= a_L m^2 - b_L m \\
a_R &= 0 \\
b_R &= -2a_R m \\
c_R &= a_R m^2 - b_R m
\end{aligned} \tag{15}$$

where $m = \dfrac{(y_{new} - y_{last})}{n}$ when n is the conversion factor.

The A matrix is defined as

$$A_{[i,j]} = \frac{\partial f_{[i]}}{\partial x_{[j]}}(\hat{x}_{k-1}^{-}, u_{k-1}) \tag{16}$$

where f are the equations of motion in discrete time, x is the state vector, and u are the inputs to the system. The state covariance matrix is updated with

$$P_k^{-} = A_k P_{k-1} A_k^T + Q_{k-1} \tag{17}$$

MEASUREMENT UPDATE

The measurement update receives coefficient, lateral distance, and longitudinal velocity measurements if a lane is detected. When both lanes are detected, the H matrix is as follows:

$$H = \begin{bmatrix}
1 & 0 & 0 & 0 & 0 & 0 & 0 & 0 & 0 & 0 & 0 \\
0 & 1 & 0 & 0 & 0 & 0 & 0 & 0 & 0 & 0 & 0 \\
0 & 0 & 1 & 0 & 0 & 0 & 0 & 0 & 0 & 0 & 0 \\
0 & 0 & 0 & 1 & 0 & 0 & 0 & 0 & 0 & 0 & 0 \\
0 & 0 & 0 & 0 & 1 & 0 & 0 & 0 & 0 & 0 & 0 \\
0 & 0 & 0 & 0 & 0 & 1 & 0 & 0 & 0 & 0 & 0 \\
0 & 0 & 0 & 0 & 0 & 0 & 1 & 0 & 0 & 0 & 0 \\
0 & 0 & 0 & 0 & 0 & 0 & 0 & 0 & 0 & 0 & 1
\end{bmatrix} \tag{12}$$

In the case of a single lane being detected, the other lane states are unobservable and the H matrix is modified to

$$H = \begin{bmatrix}
1 & 0 & 0 & 0 & 0 & 0 & 0 & 0 & 0 & 0 & 0 \\
0 & 1 & 0 & 0 & 0 & 0 & 0 & 0 & 0 & 0 & 0 \\
0 & 0 & 1 & 0 & 0 & 0 & 0 & 0 & 0 & 0 & 0 \\
0 & 0 & 0 & 0 & 0 & 0 & 1 & 0 & 0 & 0 & 0 \\
0 & 0 & 0 & 0 & 0 & 0 & 0 & 0 & 0 & 0 & 1
\end{bmatrix} \tag{13}$$

in the case where only the left lane is detected or

$$H = \begin{bmatrix}
0 & 0 & 0 & 1 & 0 & 0 & 0 & 0 & 0 & 0 & 0 \\
0 & 0 & 0 & 0 & 1 & 0 & 0 & 0 & 0 & 0 & 0 \\
0 & 0 & 0 & 0 & 0 & 1 & 0 & 0 & 0 & 0 & 0 \\
0 & 0 & 0 & 0 & 0 & 0 & 1 & 0 & 0 & 0 & 0 \\
0 & 0 & 0 & 0 & 0 & 0 & 0 & 0 & 0 & 0 & 1
\end{bmatrix} \tag{14}$$

if only the right lane is detected. If both lanes are not detected, no measurement update is conducted.

EXPERIMENTAL RESULTS

Experimental data was obtained from a highway scenario in which a single camera (a QuickCam Pro 9000) was mounted to the roof of a vehicle. The video recorded for this run has shadows crossing the road, which creates a non-ideal situation for the camera due to the increased number of candidate lines, as seen in Fig. 5. Additionally, an overpass creates a situation where both lines are not detected and the system runs solely from the IMU for several frames. The images' width and height are 245x70 pixels after the region of interest was selected prior to processing. The vehicle moves in a forward path within a single lane – no curves or lane changes were conducted. The right lane marking alternates between a solid lane

marking and a dashed lane marking (when an exit is passed). The left lane marking remains dashed for the extent of the video. As such, measurement updates for the left lane marking are much less frequent than that for the right lane marking.

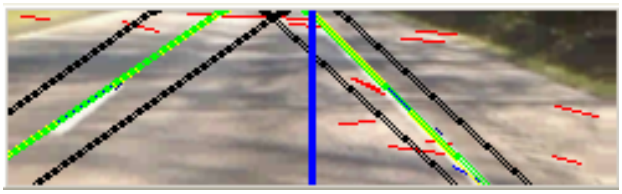

Figure 5: Image frame of video

The IMU used in the experiment was an XBOW 440 automotive grade MEMS IMU. The IMU was mounted in the center console of the vehicle. Fig. 6 shows the lateral acceleration from the IMU as well as the estimate of the bias. Around 30 seconds in the figure, the lateral acceleration "arches". This causes the estimate of the position and therefore the lateral position change (in image space) to shift.

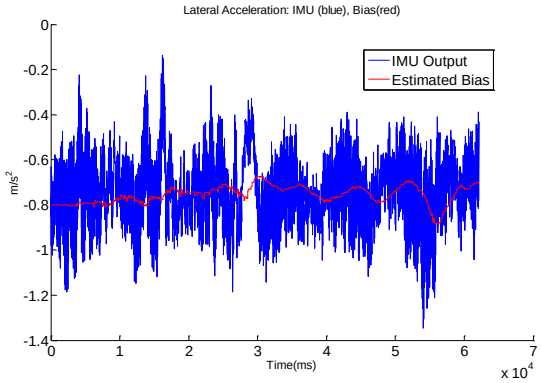

Figure 6: Lateral Acceleration from the IMU: IMU Output (blue), Bias (red)

Fig. 7 shows this lateral position shift. It is the amount in pixels that the time update shifts the left and right models of the lane markings. The arch in Fig. 6 is noticeable in Fig. 7 and serves as an example of what can happen if the bias is not estimated correctly. Within this "arch" of Fig. 7, the lane shifts several pixels until a new measurement update forces the shift back to zero.

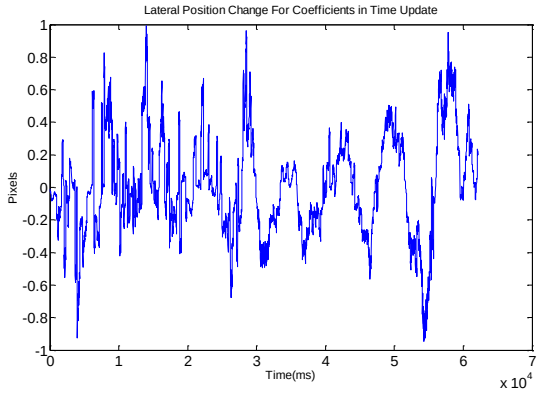

Figure 7: Lateral Position Change in Image Space for Coefficients in the Time Update

Fig. 8 shows the relationship between the estimated position from the updated IMU and the camera measured distance from the states of the estimated lane models – generally taken from the most updated lane model- the right lane model. The camera measured distance using the estimated lane models show the effect of erroneous lines within the image in the spikes of the camera measured distance. These spikes in the graph are situations where the model shifts away from the true lane marking. Most of these errors are soon followed by correct lane marking models due to the polynomial bounds and slope filter. Note that this distance for the camera measured distance was obtained by subtracting the distance to the lane by the initial position of the vehicle at the start of the run to align the plot with the estimated position from the lateral acceleration of the IMU. Similar results are obtained with the left distance from the camera.

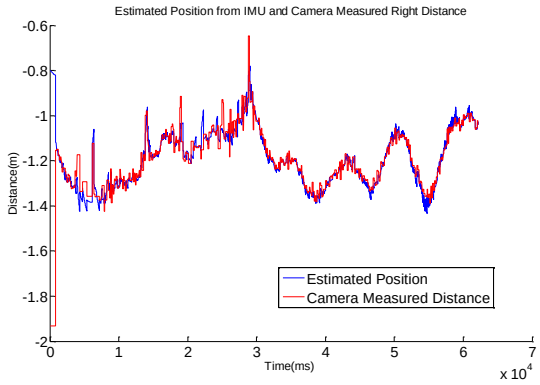

Figure 8: Estimated Position and Camera Measured Distance

Due to the use of real highway data, no survey was done for truth. Fig. 9 shows the results of the left and right distance measurements, where the right and left distances are absolute values of the number of pixels to each corresponding lane marking. Since lanes generally have constant width, an estimate of the accuracy of the system

can be obtained. From the bottom row of the image, a road within the image is typically 200 pixels wide. As seen in Fig. 9, the sum of the left and right distances hover around 200 pixels with an average of 197 pixels and a standard deviation of 9 pixels. Erroneous spikes, such as that at around 40 seconds, are due to the dashed left lane markings where measurements were less frequent.

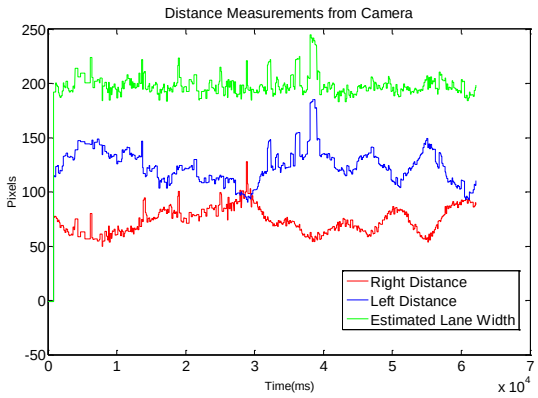

Figure 9: Distance Measurements from Camera (Right – red, Left – blue, Sum – green)

CONCLUSIONS AND FUTURE WORK

This paper has presented a technique for determining lateral position within the lane using a low resolution camera and an IMU for a vehicle. The use of a least squares interpolated polynomial for the lane model for tracking allows for a lower resolution since landmarks are not tracked across multiple images. In addition, no range measurements are needed with the use of the near range row of the image for camera distance measurement and a known image plane to real world conversion factor. This system provides a more robust system for location within the lane than a camera alone since lateral distance can be estimated even when one or both lane models are not detected in the image.

Despite these advantages, the system presented here has its own drawbacks. Longitudinal velocity cannot be updated using the polynomials for lane models since little information can be obtained from the lane marking models in the forward direction. As such, the forward velocity measurements must come from another sensor. Fortunately, speedometers can provide this measurement and is already present in vehicles. The bias in the lateral acceleration is very important in the estimate of velocity and position and can create problems if not estimated correctly. If the mean of the lateral acceleration is not zero, then the position estimate will likely drift away, and the polynomial models of the lanes will drift off of the image, further preventing the bias from being correctly estimated. Fortunately, this situation is easily detected and the lane model can be reset to search for the lane within the image. The current means of determining the movement of the lane within the image when no lane is detected in the image is limited to a horizontal shift of the polynomial based on the lateral position change from the lateral acceleration of the IMU. Certainly, lane markings within the image do no move in this manner when the vehicle shifts in the lane or changes lanes. For a straight road, the lane marking extends out to the vanishing point on the horizon regardless of its position within the image; thus, large shifts without a measurement update will produce an erroneous lane model in all but the point of measurement on the lowest row of the image. The use of the lowest row of the image as the measurement of distance is highly dependent on the assumption that no skew or lens distortion is present and that each pixel corresponds to the conversion factor. Future work entails finding solutions for these problems.

ACKNOWLEDGMENTS

The Federal Highway Administration is funding this project and others across the range of issues that are critical to the transportation industry through the Exploratory Advanced Research (EAR) Program. For more information, see the EAR Web site at http://www.fhwa.dot.gov/advancedresearch/about.cfm#focus

REFERENCES

[1] J. Allen, J. Britt, C. Rose, and D. Bevly, “Intelligent Multi-Sensor Measurements to Enhance Vehicle Navigation and Safety Systems”, Proceedings of the 2009 International Technical Meeting, Anaheim, California.

[2] A. Ansar and K. Daniilidis, “Linear Pose Estimation from Points or Lines”, in *IEEE Transactions on Pattern Analysis and Machine Intelligence*, May 2003, pp. 578-589.

[3] L. Armesto, S. Chroust, M. Vincze, and J. Tornero, “Multi-rate Fusion with Vision and Inertial Sensors”, in *Proceedings of the 2004 IEEE International Conference on Robotics and Automation*, 2004, pp.193-199.

[4] L. Armesto, J. Tornero, and M. Vincze, “Fast Ego-motion Estimation with Multi-rate Fusion of Inertial and Vision”, in *The International Journal of Robotics Research*, June 2007, vol. 26, no.6, pp. 577-589.

[5] J. Britt and D. Bevly, “Lane Tracking using Multilayer Laser Scanner to Enhance Vehicle Navigation and Safety Systems”, Proceedings of the 2009 International Technical Meeting, Anaheim, California.

[6] T. Broida, S. Chandrashekhar, and R. Chellapa, "Recursive 3-D Motion Estimation from a Monocular Image Sequence", in *IEEE Transactions on Aerospace and Electronic Systems*, July 1990, vol. 26, no. 4, pp. 639-656.

[7] P. Chalimbaud, F. Marmoiton, and F. Berry, "Towards an Embedded Visuo-Inertial Smart Sensor", in *The International Journal of Robotics Research*, June 2007, vol. 26, no. 6, pp. 537-546.

[8] P. Corke, J. Lobo, and J. Dias, "An Introduction to Inertial and Visual Sensing", in *The International Journal of Robotics Research*, June 2007, vol. 26, no.6, pp. 519-535.

[9] E. Dickmanns and B. Mysliwetz, "Recursive 3-D road and relative ego-state recognition", in *IEEE Transactions on Pattern Analysis and Machine Intelligence*, February 1992, vol. 14, pp. 199-213.

[10] Y. Feng, W. Rong-ben, and Z. Rong-hui, "Based on digital image lane edge detection and tracking under structure environment for autonomous vehicle", in *IEEE International Conference on Automation and Logistics*, August 2007, pp. 1310-1314.

[11] P. Gemeiner, P. Einramhof, and M. Vincze, "Simultaneous Motion and Structure Estimation by Fusion of Inertial and Vision Data", in in *The International Journal of Robotics Research*, June 2007, vol. 26, no. 6, pp. 591-605.

[12] A. Gern, R. Moebus, and U. Franke, "Vision-based lane recognition under adverse weather conditions using optical flow", in *IEEE Intelligent Vehicle Symposium*, June 2002, vol. 2, pp. 17-21.

[13] P. Hsiao and C. Yeh, "A portable real-time lane departure warning system based on embedded calculating technique", in *Vehicular Technology Conference*, May 2006, vol. 6, pp. 2982-2986.

[14] C.R. Jung and C.R. Kelber, "A lane departure warning system using lateral offset with uncalibrated camera", in *Intelligent Transportation Systems*, September 2005, pp. 102-107.

[15] C.R. Jung and C.R. Kelber, "A lane departure warning system based on a linear-parabolic lane model", in *IEEE Intelligent Vehicles Symposium*, June 2004, pp. 891-895.

[16] D. Khosla, "Accurate estimation of forward path geometry using two-clothoid road model", in *IEEE Intelligent Vehicle Symposium*, June 2002, vol. 1, pp. 154-159.

[17] S. Kim and S. Oh, "A Driver Adaptive Lane Departure Warning System Based on Image Processing and a Fuzzy Evolutionary Technique", in *IEEE Intelligent Vehicle Symposium*, June 2003, vol. 1, pp. 361-365.

[18] C.-K. Lee, R.M. Haralick, and K. Deguchi, "Estimation of curvature from sampled noisy data", in *Computer Vision and Pattern Recognition*, June 1993, pp. 536-541.

[19] S. Lee, W. Kwon, and J.-W. Lee, "A vision based lane departure warning system", in *IEEE/RSJ International Conference on Intelligent Robots and Systems*, October 1999, vol. 1, pp. 160-165.

[20] J. Lobo and J. Dias, "Relative Pose Calibration Between Visual and Inertial Sensors", in *The International Journal of Robotics Research*, June 2007, vol. 26, no. 6, pp. 561-575.

[21] S. Mahmoud, M. Afifi, and R. Green, "Identification and Velocity Computation of Multiple Moving Objects in Images", in *IEEE Transactions on Aerospace and Electronic Systems*, July 1990, vol. 26, no. 4, pp. 586-598.

[22] G. Mariottini, G. Pappas, D. Prattichizzo, and K. Daniilidis, "Vision-based Localization of Leader-Follower Formations", in *Proceedings of the 44th IEEE Conference on Decision and Control*, and the European Control Conference, 2005, pp. 635-640.

[23] F. Mirzaei and S. Roumeliotis, "A Kalman Filter Based Algorithm for IMU-Camera Calibration: Observability Analysis and Performance Evaluation" in IEEE *Transactions on Robotics*, October 2008, vol. 24, no. 5, pp. 1143-1156.

[24] H. Rehbinder and B. Ghosh, "Pose estimation using line-based dynamic vision and inertial sensors" in *IEEE Transactions on Automatic Control*, February 2003, vol. 48, issue 2, pp. 186-199.

[25] C. Rose and D. Bevly, "Vehicle Lane Position Estimation with Camera Vision using Bounded Polynomial Interpolated Lines" in Proceedings of the 2009 International Technical Meeting, Anaheim, California.

[26] D. A. Schwartz, "Clothoid road geometry unsuitable for sensor fusion clothoid parameter sloshing", in *Intelligent Vehicles Symposium*, June 2003, pp. 484-488.

[27] A. Takahashi and Y. Ninomiya, "Model-based lane recognition", in *Proceedings of the 1996 IEEE Intelligent Vehicles Symposium*, September 1996, pp. 201-206.

[28] C. Tomasi, and J. Shi, “Good Features to Track”, in *Proceedings of the IEEE Computer Society Conference on Computer Vision and Pattern Recognition*, June 1994, pp. 593-600.

[29] Jin Wang, S. Schroedl, K. Mezger, R. Ortloff, A. Joos, and T. Passengger, “Centimeter vehicle positioning and lane keeping”, in *Intelligent Transportation Systems*, 2003, vol. 1, pp. 649-654.

[30] “Roadway Depature Safety,” FHWA Safety, December 9, 2008. [Online]. Available: http://safety.fhwa.dot.gov/roadway_dept/ [Accessed: Jan 29, 2009].